Cancer Chemotherapy and Pharmacology (2026) 96:22
https://doi.org/10.1007/s00280-026-04870-4

ORIGINAL ARTICLE

Window of opportunity study measuring defactinib and avutometinib delivery in glioblastomas

Miguel Mayol Del Valle[1] · Emely Morales Colon[2] · Kavitha Kettimuthu[3] · Kristal Maner-Smith[3] · Jeffrey J. Olson[4] · Lilia Y. Kucheryavykh[2]

Received: 21 October 2025 / Accepted: 7 February 2026

Abstract

Purpose Glioblastoma (GBM) is the most common malignant brain tumor in adults, and durable control or cure with current standard or investigational therapies is rare. Therefore, novel approaches are needed. This exploratory study evaluated whether defactinib and avutometinib, inhibitors of FAK/Pyk2 and RAF/MEK signaling respectively, penetrate GBM and produce measurable effects on their molecular targets.

Methods Defactinib or avutometinib was administered to six subjects each, in two escalating dose levels: avutometinib at 3.2 mg and 4 mg, and defactinib at 200 mg and 400 mg (three patients per dose level). Administration occurred immediately prior to craniotomy for tumor resection. Tumor tissue, peritumoral brain tissue, and blood were collected during surgery. Drug concentrations were measured by liquid chromatography–mass spectrometry, and effects on the intended molecular targets were assessed by western blot analysis.

Results Even after a single preoperative dose, both defactinib and, to a lesser extent, avutometinib were detectable in tumor tissue 3–4 h after administration. Peritumoral brain tissue contained lower concentrations of each agent. Exploratory pharmacodynamic analyses suggested target engagement: avutometinib (3.2 mg) reduced Erk1/2 phosphorylation approximately 28-fold, while defactinib (400 mg) reduced Pyk2 phosphorylation by 5.7-fold within tumor tissue. Effects in peritumoral tissue were minimal.

Conclusion These exploratory findings demonstrate that defactinib and avutometinib can penetrate GBM tissue and produce measurable modulation of their intended molecular targets after a single dose, with limited impact on surrounding brain. While the small sample size and inherent tissue heterogeneity limit definitive conclusions, this study supports the feasibility of presurgical pharmacokinetic and pharmacodynamic evaluation in GBM and provides a rationale for further clinical studies to optimize dosing, target inhibition, and therapeutic efficacy.

Trial Registration Number ClinicalTrials.gov NCT05798507. Date of Registration March 3, 2023.

Keywords Defactinib · Avutometinib · Glioblastoma · Window of opportunity

Introduction

Though glioblastomas (GBM) are not common (3.27 per 100,000 population), they account for 13.9% of all central nervous system tumors and 51.5% of the malignant tumors arising from the central nervous system. Prognosis is poor for people with GBM, with a median overall survival of 9 months and a 5-year survival rate of 7.1% [1].

Despite substantial advances in understanding the molecular biology of gliomas, this knowledge has not translated into clearly effective targeted therapies. For example, vorasidenib, which targets IDH1/2 mutations, represents a meaningful advance [2, 3]. Bevacizumab, an anti-VEGF

✉ Lilia Y. Kucheryavykh
lilia.kucheryavykh@uccaribe.edu

1 Department of Neurosurgery, University of Puerto Rico Medical Sciences Campus, San Juan, Puerto Rico, USA

2 Department of Biochemistry, Universidad Central del Caribe, Bayamon, PR, USA

3 Emory Integrated Metabolomics and Lipidomics Core, Emory University School of Medicine, Atlanta, GA, USA

4 Department of Neurosurgery, Emory University School of Medicine, Atlanta, GA, USA

Published online: 06 March 2026

therapy, failed to improve overall survival in patients with GBM [4, 5]. Similarly, substantial resources have been directed to targeting the Epidermal Growth Factor Receptor (*EGFR)* signaling pathway in newly diagnosed and progressive GBM, with no reliable and reproducible benefit being identified [6–8]. While MGMT promoter methylation is prognostically significant in GBM treated with alkylating chemotherapy, no effective therapies directly targeting this alteration have been developed [9]. Moreover, given the well-recognized issue of reporting bias, it is likely that numerous unsuccessful clinical trials targeting molecular abnormalities in GBM remain unpublished.

It is recognized that the development of novel treatment agents for GBM does not include assessment of their ability to reach their targets in the central nervous system [10]. Skipping this critical step may account for the failure of some clinical trials that otherwise seem grounded in good science.

Previous studies have identified deregulation of Focal adhesion kinases 1 and 2 (*FAK and Pyk2)* and *RAF/MEK* signaling in human GBMs. This deregulation is frequently driven by overactivation and gain of gene copy number of their upstream receptor tyrosine kinases, including *EGFR*, Platelet-Derived Growth Factor receptor (*PDGFR)*, and *Fibroblast Growth Factor Receptor (FGFR)* receptor tyrosine kinases [11, 12]. Although oncogenic driver mutations in KRAS and BRAF are uncommon in GBM, the presence of BRAF V600 mutations, upregulation of BRAF and RAF-1, and alterations in Neurofibromatosis Type 1 (NF1), a negative regulator of Ras signaling, have been reported in GBM, all contributing to downstream effects on KRAS-related tumorigenesis [13–17]. In vivo GBM studies demonstrate that MEK inhibitors such as trametinib and selumetinib can slow tumor growth and modestly extend survival in orthotopic models [18–19]. However, their efficacy is limited by feedback activation of compensatory signaling pathways.

FAK and Pyk2 act as critical signaling effectors that promote glioma cell proliferation, migration, and survival [20–21]. FAK primarily regulates proliferative signaling, whereas Pyk2 is involved in glioma cells invasion [22–25]. Our previous findings demonstrated that cytokines released by tumor-infiltrating myeloid cells activate Pyk2 at Tyr579/580 and FAK at Tyr925, promoting glioma cell proliferation and dispersal [12], suggesting that pharmacologic inhibition of Pyk2 and FAK may provide therapeutic benefit in GBM. Consistent with this hypothesis, our preclinical studies using primary human GBM cell lines showed that combined pharmacological inhibition of FAK/Pyk2 and temozolomide (TMZ) significantly enhanced TMZ efficacy, resulting in reduced cell viability, impaired cell-cycle progression, and decreased invasion and invadopodia formation compared with TMZ alone [26]. In in vivo studies using the GL261/C57BL/6 glioma implantation model the combinatorial treatment led to prominent reductions in tumor size and invasive margins, increased apoptosis, reduced proliferation index, and a 15% improvement in survival compared with TMZ monotherapy [26]. In addition, the FAK/Pyk2 inhibition with PF-562,271 suppressed recurrent tumor growth in mouse glioma implantation model [27]. Supporting the clinical relevance of these findings, analysis of microarray data from 619 GBM patients in The Cancer Genome Atlas revealed significantly improved survival in individuals with low Pyk2 gene expression ($p=0.009$) as well as low FAK gene expression ($p=0.0275$), compared with those showing high expression of either gene [27].In another cancer type, low-grade serous ovarian carcinoma, the combined inhibition of RAF and FAK with avutometinib and defactinib has shown efficacy in animal models and in a phase II clinical trial, where an objective response rate of 42.3% was observed [28–29]. This is encouraging, as both serous ovarian carcinoma and GBM share activation of the RAS/RAF/MEK/ERK growth pathway [30]. Collectively, these findings suggest that RAF and FAK signaling represent promising therapeutic targets in GBM. However, prior clinical trials testing inhibitors of FAK/Pyk2 or RAF signaling individually have identified only modest improvements in progression-free survival [31–32].

Mechanistically, compensatory upregulation of FAK/Pyk2 signaling has been observed in response to RAF inhibition, driving treatment resistance. In contrast, co-inhibition of BRAF and FAK/Pyk2 prevented compensatory Erk reactivation, resulting in improved tumor growth control [33]. FAK can promote Ras activity through competitive recruitment of p120RasGAP [24], and integrin–FAK signaling has been shown to sustain MEK/ERK activity [34]. These findings indicate that FAK/Pyk2-driven signaling networks function as a common compensatory resistance mechanism in GBM. Notably, GBM cells lacking FAK are markedly more sensitive to MEK inhibitors, including trametinib and GDC0623, than FAK-wildtype cells [35]. In an orthotopic human G7 glioma model, trametinib or the FAK inhibitor VS-4718 alone produced only modest tumor regression, whereas the combined treatment resulted in dramatic tumor reduction [35]. Thus, dual MEK and FAK/Pyk2 inhibition yields substantially greater antitumor efficacy than either approach alone.

Based on this, we hypothesize that dual inhibition of *RAF/MEK* and *FAK/Pyk2* signaling through the combined administration of avutometinib and defactinib will suppress GBM tumor cell proliferation and may represent a novel therapeutic strategy. Avutometinib and defactinib, are next-generation inhibitors with distinct pharmacologic properties, improved tolerability, and enhanced target engagement compared with earlier MEK and FAK/Pyk2 inhibitors. As an

initial step, we assessed the delivery and molecular effects of single-agent administrations of avutometinib and defactinib in subjects with GBM. These findings will provide the foundation for future development of combinatorial therapies targeting Pyk2/FAK and RAF/MEK signaling in GBM.

Materials and methods

This study is a single-dose, presurgical, window of opportunity, alternating-agent, two-dose-level clinical trial. The primary endpoint was to determine whether defactinib and avutometinib reached GBM tissue following oral administration. Secondary endpoints included assessment of pharmacodynamic target engagement within tumor samples, as measured by phosphorylation changes in targeted signaling proteins, as well as evaluation of drug presence in plasma and tumor-adjacent brain tissue.

Enrollment criteria

Potentially eligible subjects were identified through the neurosurgery and oncology inpatient and outpatient services of Emory University Winship Cancer Institute, in accordance with informed consent procedures approved by the Emory Institutional Review Board (IRB) and Research and Healthcare Compliance Offices (STUDY00004876). Additionally, frozen control human GBM tissue samples were obtained from the Universidad Central del Caribe (UCC) GBM specimen collection, with patient consent for future use of de-identified tissue, as approved by the UCC IRB Human Research Subject Protection Office (protocol # 2012-12B). In total, eight control GBM samples from the UCC collection were analyzed.

The primary eligibility requirement was the presence of a new or recurrent GBM suggested by imaging, for which surgical resection was indicated. Under the Emory IRB–approved protocol, subjects signed informed consent prior to undergoing formal screening for eligibility.

Inclusion criteria required participants to be ≥21 years of age with an Eastern Cooperative Oncology Group (ECOG) performance status of 1 or better. Standard laboratory parameters had to be within acceptable ranges. Baseline QTc interval on electrocardiogram was required to be ≤460 ms for women and ≤450 ms for men (average of triplicate readings), using Fredericia's QT correction formula.

Exclusion criteria included pediatric patients, pregnancy, prisoners, clinically significant active gastrointestinal abnormalities, requirement for systemic anticoagulation or potent cytochrome CYP2C8 inhibitors, a history of significant cardiac or pulmonary disorders, hepatitis B or C, HIV infection, actively treated glaucoma, retinal vein occlusion, or any form of active corneal erosion.

Drug administration plan

The potential value of combining defactinib and avutometinib has been investigated in low-grade serous ovarian cancer using defactinib 200 mg twice daily and avutometinib 3.2 mg twice weekly [29, 33]. To minimize the risk of excessive toxicity, initial dosing in this study was limited to single administrations at conservative starting levels. A second, higher dose level was planned to assess whether greater drug delivery or biologic effects could be achieved. In the first cohort, three subjects received defactinib 200 mg and three received avutometinib 3.2 mg, with treatments administered in an alternating fashion. No dose-limiting toxicities were observed. Consequently, a second cohort of six subjects was treated with higher doses—defactinib 400 mg and avutometinib 4.0 mg—again administered alternately as in the initial cohort (Fig. 1).

The study drugs were administered orally 1–2 h prior to surgery. Craniotomy was then performed in a standard manner according to tumor location utilizing MRI-based image guidance and optical magnification to confirm proper navigation to the target lesion. Tumor tissue samples, approximately 1.5–2.0 cm^3 in size, were obtained from three separate non-necrotic regions within the tumor mass. Each specimen was immediately placed into a tube containing ice-cold phosphate-buffered saline (PBS) and subsequently stored at −80 °C until further analysis. The time of sample collection was recorded for each specimen.

Similarly, adjacent non-eloquent brain tissue samples (deemed to be tumor-infiltrated brain), approximately 0.25–0.5 cm^3 in size, were collected, and the timing of sampling was recorded. In addition, a 10 ml blood sample was obtained intraoperatively to measure plasma concentrations of defactinib or avutometinib, with the time of collection documented (Fig. 2).

After tissue sampling, all subsequent care was provided according to standard clinical practice, and subjects were taken off study at the time of staple or suture removal. During this interval, patients were monitored for toxicity. Molecular data, including tumor mutation panels and RNA sequencing microarray data, were obtained from the Emory Department of Neuropathology to provide additional correlative support.

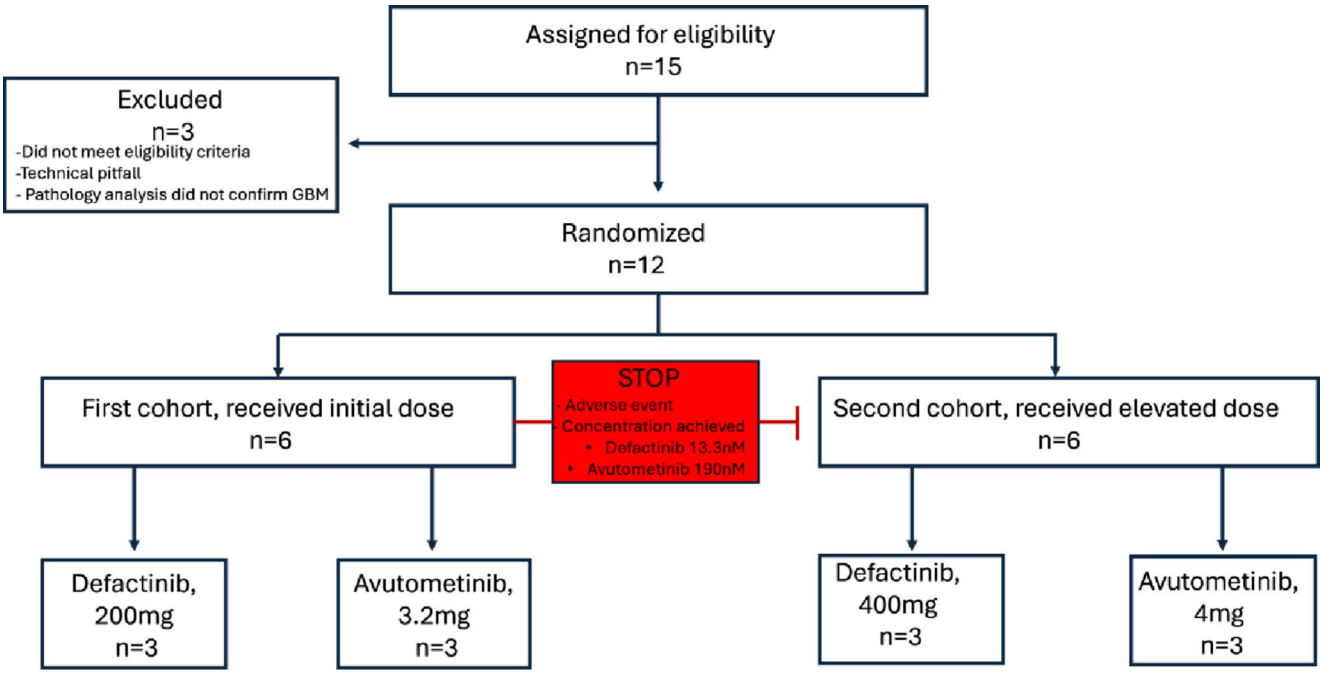

Fig. 1 Clinical Trial design: dose-escalation and cohort allocation

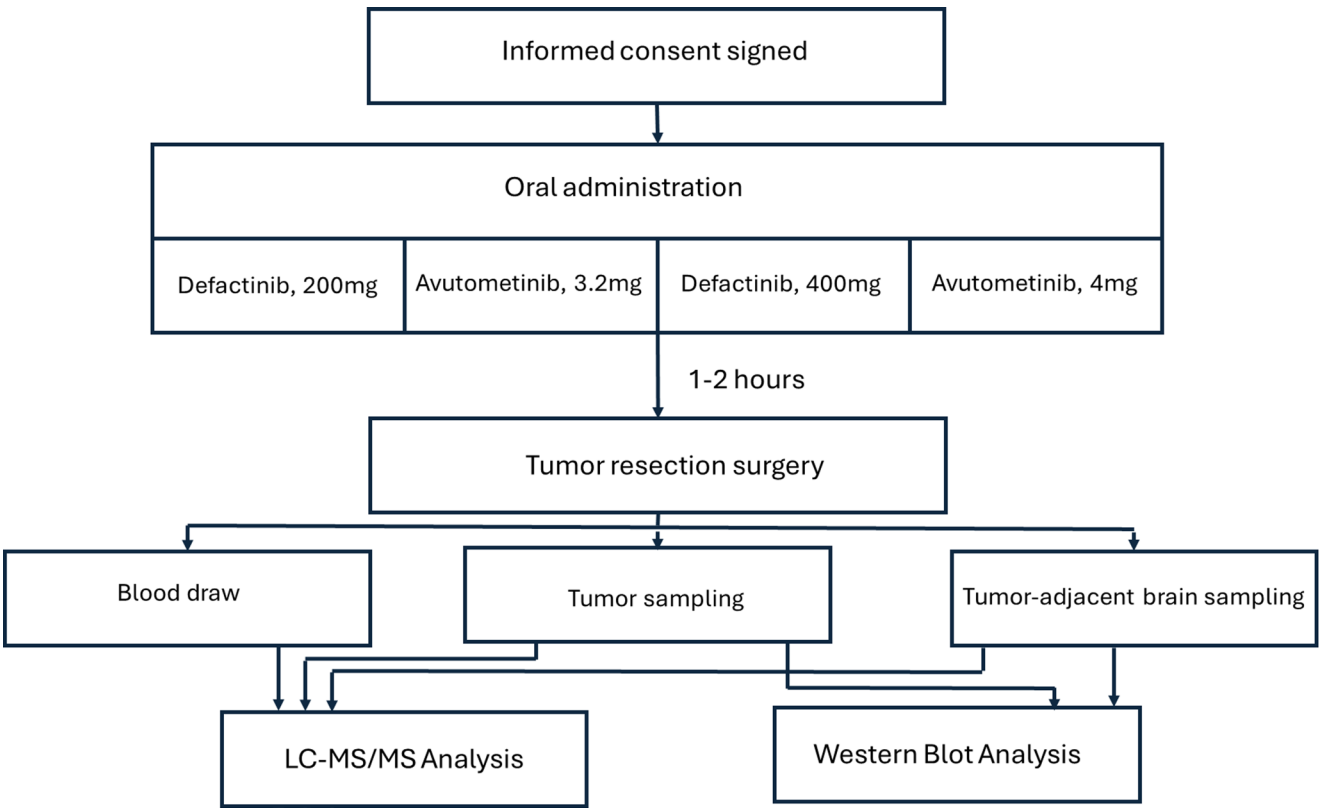

Fig. 2 Workflow of drug administration, sample collection, and analysis protocol

Quantification of defactinib (VS-6063) and avutometinib (VS-6766) in human plasma and brain tissue using liquid chromatography-mass spectroscopy/mass spectroscopy (LC-MS/MS)

Sample preparation and extraction

Defactinib, it's M2 (N-desmethyl sulfonamide), and M4 (N-desmethyl amide) metabolites (Investigators Brochure, Edition 16, Verastem, Inc.) and Avutometinib in human plasma and brain and tumor tissue were quantified using an LC-MS/MS assay developed at the Integrated Lipidomics and Metabolomics Core Laboratory, Emory University School of Medicine.

Briefly, sample preparation involved protein precipitation using a two-step solvent approach. Each sample was dissolved in DMSO and centrifuged at 4,000×g for 5 min at 4 °C. Supernatant was transferred to a 96-well plate and mixed with an equal volume of methanol. A second centrifugation was performed under the same conditions, and the final clear supernatant was used for LC-MS/MS analysis.

To generate a Global QC (quality control) sample, 10 µL aliquots from each individual study sample were pooled either prior to extraction (from original samples) or post-extraction (after supernatant collection). The pooled QC was processed using the same protocol and analyzed alongside study samples. Spiked recovery studies were conducted using Standard Reference Material (SRM 1950) plasma to assess accuracy and precision. Known concentrations of analytical standards were spiked into SRM 1950, and the measured concentrations were compared with the concentrations of the reference standards.

LC-MS/MS analysis high-performance liquid chromatography (HPLC)

Chromatographic separation was achieved using a SCIEX Exion LC system equipped with a Thermo Scientific Accucore™ C18 column (100 × 4.6 mm, Part No. 17126–104630). The mobile phase consisted of 0.1% formic acid in water and 0.1% formic acid in methanol, delivered at a flow rate of 1.0 mL/min. The column was maintained at 40 °C, and the injection volume was 15 µL. A 5.5-minute gradient elution was employed as per Online Resource 1.

Mass spectrometric detection was performed using a SCIEX QTRAP 5500 operated in positive ionization mode.

For calibration of the drug and associated metabolites, analytical grade calibration standards were prepared between 0.1 and 50 µg/ml. The calibration curve demonstrated good linearity between 0.1-10µg/ml, with R2 values > 0.90. Using the signal-to-noise (S/N) ratio to determine the LLOD and LLOQ, the LLOD and LLOQ were calculated to be above 3.3x and 10x noise levels, respectively (Online Resource 2). Based on these calculations, the LLOQ was determined to be 0.03 µg/mL and the LLOD to be 0.01 µg/mL in both brain and plasma.

As mentioned above, the compounds analyzed included: VS-6063 and VS-6766, along with VS-6063 metabolites M2 and M4. The following MRM transitions (Q1 & Q3) were used for ion extraction as per Online Resource 3.

Data analysis

Instrument parameters were optimized using reference standard solutions. Peak detection, integration, and calibration curve generation were performed using Skyline software. Quantification was based on linear regression analysis of the calibration curves, and results were reported as concentrations in µ g/mL.

Western blot analysis

Frozen brain and tumor tissue specimens were lysed in RIPA buffer. Protein concentrations were determined using a Bradford assay kit (Bio-Rad, cat. #5000006). A 30-µg protein samples were resolved with 10% SDS-PAGE and transferred onto Amersham Hybond ECL nitrocellulose membranes (GE Healthcare Bio-Sciences Corp., Pittsburgh, PA, USA). The antibodies used in this study were developed against p-Pyk2[Y579/Y580] (1:500, Invitrogen, Carlsbad, CA, USA, cat. # 44-636G), Pyk2 (1:1000), p-FAK[Y925] (1:1000), FAK (1:1000), Erk1/2 (1:1000), p-Erk1/2[Thr202/Tyr204], MEK1/2, p-MEK1/2[Ser217/221] (Cell Signaling Technology, Danvers, MA, USA, cat. #3292, #3284, #3285, #4696, #4370, #4694, #9154, respectively). GAPDH (Cell Signaling Technology, Danvers, MA, USA, cat. # 97166) immunoreactive signal was used as the loading control. The signals were visualized using the Odyssey CLx Quantitative Infrared Imaging System with the corresponding secondary infrared antibodies IRDye 800CW goat anti-rabbit and IRDye 680RD goat anti-mouse (1:25,000, LI-COR Biotechnology, cat. #925-32211, #926-68070). Results were analyzed with Image Studio Lite Software (LI-COR Biotechnology).

Statistical analysis

Data are presented as mean ± standard deviation (SD). Statistical comparisons were performed with two-way analysis of variance (ANOVA). The p-value of < 0.05 was considered significant. When a significant overall effect was present, intergroup comparisons were performed using a Tukey–Kramer correction for multiple comparisons in GraphPad Prism 9.1.0 statistical software (San Diego, CA, USA).

Table 1 Avutometinib concentrations in brain and tumor samples

Manuscript subject name	Avutometinib dose (mg)	Mean avutometinib concentration (µg/ml)+/- SD In tumor	Avutometinib concentration (µ g/ml) In brain
2	3.2	0.004+/-0.004	0.006
4	3.2	0.001+/-0.001	0.005
6	3.2	0.002+/-0.002	0.006
7	4	0.003+/-0.002	0.005
10	4	0.004+/-0.003	0.006
12	4	0.001+/-0.002	0

Results

Subject demographics

A total of 15 subjects signed informed consent to participate in the study. One was excluded due to ineligibility, and one did not receive the preoperative investigational drug because of technical issues in the research pharmacy. In one individual, the lesion was found to be an infarction rather than a glioblastoma. Thus, twelve subjects completed the study and provided data for analysis.

Of these, six received avutometinib—three at 3.2 mg and three at 4.0 mg—and six received defactinib—three at 200 mg and three at 400 mg (Fig. 1). Among the eligible subjects who completed the study, the mean age was 62.4 years (range 24–76 years), and five were female. Demographic details are summarized in Online Resource 4.

Drug concentrations analysis

Avutometinib analysis

Plasma: Avutometinib was not measurable in plasma after the 3.2 mg dose or the 4 mg dose. The time interval from drug ingestion to plasma sampling ranged from 183 to 264 min.

Tumor-Infiltrated Brain: Avutometinib was detected in all samples from subjects receiving the 3.2 mg dose, with concentrations ranging from 0.005 µg/ml to 0.006 µg/ml. In the 4.0 mg dose group, drug was detected in 2 of the 3 subjects, with concentrations of 0.005 µg/ml and 0.006 µg/ml. The interval between drug administration and tissue sampling ranged from 156 to 319 min (Table 1).

Brain Tumor: Three samples were taken from different regions of each tumor to account for expected intralesional heterogeneity; drug concentrations are therefore reported as mean values. For the 200 mg dose of defactinib, mean concentrations ranged from 0.001 µg/ml to 0.004 µg/ml. For the 400 mg dose, mean concentrations were within the same range (0.001 µg/ml to 0.004 µg/ml). As shown in Table 1, the standard deviations were sufficiently large to indicate that concentrations at the 200 mg and 400 mg doses were not significantly different. The interval between drug administration and tissue sampling ranged from 176 to 255 min for the 3.2 mg dose and from 151 to 256 min for the 4 mg dose.

Defactinib analysis

Plasma: In the three subjects receiving the 200 mg dose of defactinib prior to surgery, measured concentrations ranged from 0.01 to 0.04 µg/ml, with a time interval from ingestion to sampling of 151 to 212 min. Among the three subjects receiving the 400 mg dose, only one had a measurable concentration of 0.02 µg/ml, with the time interval from ingestion to sampling ranging from 146 to 189 min.

Tumor-Infiltrated Brain: Defactinib was not detected in peritumoral brain tissue in all but one case, likely because the sample in that instance contained more infiltrating tumor than expected. The M2 metabolite of defactinib was detected in 4 of the 6 samples (Table 2). Among subjects receiving the 200 mg dose, M2 concentrations were 0.003 µg/ml and 0.004 µg/ml in two cases and undetectable in the third. In the 400 mg dose group, M2 concentrations were 0.002 µg/ml and 0.006 µg/ml in two cases and undetectable in the third. The M4 metabolite was detected in only one subject, at a concentration of 0.015 µg/ml, in an individual receiving the 400 mg dose. The interval between dose administration and tissue sampling ranged from 131 to 190 min.

Table 2 Defactinib concentrations in brain and tumor samples

Manuscript subject name	Defactinib dose (mg)	In tumor			In brain		
		Mean defactinib concentration (µg/ml)+/-SD	Mean M2 metabolite concentration (µg/ml)+/-SD	Mean M4 metabolite concentration (µg/ml)+/-SD	Defactinib concentration (µg/ml)	M2 metabolite concentration (µg/ml)	M4 metabolite concentration (µg/ml)
1	200	0	0.001+/-0.0014	0.0167+/-0.012	0.054	0.003	0
3	200	0.108+/-0.077	0.002+/-0.0016	0	0	0	0
5	200	0.192+/-0.272	0.003+/-0.0024	0	0	0.004	0
8	400	0	0.004+/-0.0028	0.033+/-0.04	0	0	0
9	400	0.099+/-0.138	0.003+/-0.0005	0.015+/-0.017	0	0.005	0.015
11	400	0.036+/-0.051	0.002+/-0.002	0.002+/-0.003	0	0.002	0

Brain Tumor: Three samples were taken from different regions of each tumor to account for intralesional heterogeneity; drug concentrations are therefore reported as means with standard deviations. In the 200 mg defactinib cohort, mean concentrations were 0.108 µg/ml and 0.192 µg/ml in two subjects, respectively, and undetectable in the third. In the 400 mg cohort, mean concentrations were 0.099 µg/ml and 0.036 µg/ml in two subjects, respectively, and undetectable in the third. As shown in Table 2, the standard deviations indicate that the differences in concentrations between the 200 mg and 400 mg doses are not statistically significant.

The M2 metabolite concentration ranged from 0.001 µg/ml to 0.003 µg/ml in the 200 mg cohort and from 0.002 µg/ml to 0.004 µg/ml in the 400 mg cohort. Standard deviation analysis similarly indicates no significant difference between the two dose groups. The mean M4 metabolite concentration in the 200 mg cohort was 0.0167 µg/ml in one subject and undetectable in the other two. In the 400 mg cohort, mean M4 concentrations ranged from 0.002 µg/ml to 0.033 µg/ml, with standard deviations again indicating no significant difference between doses.

The interval from drug administration to tissue sampling ranged from 145 to 215 min for the 200 mg dose and from 135 to 205 min for the 400 mg dose.

Exploratory pharmacodynamic analysis

Avutometinib downregulates Erk and MEK phosphorylation in GBM

Frozen tumor samples from three distinct tumor regions (proximal, middle, and distal), along with tumor-adjacent brain tissue, that were collected from participants who received avutometinib from 151 to 256 min prior to tumor sampling, were analyzed. Additionally, four frozen GBM specimens from the UCC collection with matching inclusion and exclusion criteria were used as untreated GBM controls. Tumor-adjacent brain tissues from participants treated with defactinib were used as controls for avutometinib-treated adjacent brain samples, due to the unavailability of untreated healthy brain tissue.

Avutometinib, administered orally at a dose of 3.2 mg 176–255 min prior to surgical tumor tissue sampling in three subjects, led to a significant 28-fold reduction in Erk1/2 phosphorylation at Thr202/Tyr204 in tumor tissues ($p = 0.0001$), with a predicted mean difference of 9.2 compared to untreated control tumors (Fig. 3a, Online Resource 5). In tumor-adjacent brain tissues, a 4-fold reduction in Erk1/2 phosphorylation was observed with a predicted mean difference of 2.6; however, this did not reach statistical significance.

A non-significant 2.5-fold reduction in p-MEK1/2 (Ser217/221) expression was observed in avutometinib-treated versus untreated tumor specimens, with no notable effect in adjacent brain tissue.

Notably, a significant 2.7-fold increase in Erk1/2 phosphorylation was detected in control GBM specimens compared to subject tumor-adjacent brain tissue, while MEK1/2 phosphorylation levels did not show a significant difference between these two groups (Fig. 3a).

Escalation of the avutometinib dose to 4 mg in three additional subjects (administered 151–256 min prior to surgical tumor tissue sampling) did not lead to further reduction in Erk1/2 or MEK1/2 phosphorylation in tumor tissue (mean reductions: 4.55 for p-Erk1/2 and 2.5 for p-MEK1/2) or adjacent brain tissue (2.8-fold for p-Erk1/2 and 2.6-fold for p-MEK1/2, Fig. 3b, Online Resource 4). However, these reductions did reach statistical significance. The lower mean reduction in the 4 mg cohort compared to the 3.2 mg cohort was attributed to one participant (Patient 7), who showed only a 2-fold reduction in Erk1/2 phosphorylation compared to the 18–28-fold reductions observed in other patients. No changes were observed in total Erk or MEK protein expression at either dose level.

When analyzing response to avutometinib based on sex, tumor location, or genetic profile, no significant differences were found. Tumors harboring PTEN, EGFR, or Rb1 mutations, as well as KRAS and BRAF amplifications, responded similarly to avutometinib.

Defactinib modulates Pyk2 phosphorylation in GBM

Tumor samples, along with tumor-adjacent brain tissue, were collected from six participants who received the Pyk2/FAK inhibitor defactinib 133–215 min prior to surgical tumor tissue sampling, as previously described. Four frozen GBM specimens from the UCC collection served as untreated GBM controls. Tumor-adjacent healthy brain tissues from participants treated with avutometinib were used as controls for defactinib-treated adjacent brain samples.

Following oral administration of 200 mg defactinib 145–215 min prior to surgical tumor tissue sampling, no significant differences in Pyk2 or FAK phosphorylation were observed in tumor or tumor-adjacent brain tissues compared to control samples (Fig. 4a). However, dose escalation to 400 mg (administered 133–205 min prior to surgical tumor tissue sampling) resulted in a significant 5.7-fold reduction in Pyk2 phosphorylation at Tyr579/580 in tumor tissue, with a predicted mean difference of 8.4 compared to untreated tumors (Fig. 2b, Online Resource 6). A 1.5-fold reduction in phosphorylation was observed in adjacent brain tissue (predicted mean difference of 3.4), although this did not reach statistical significance.

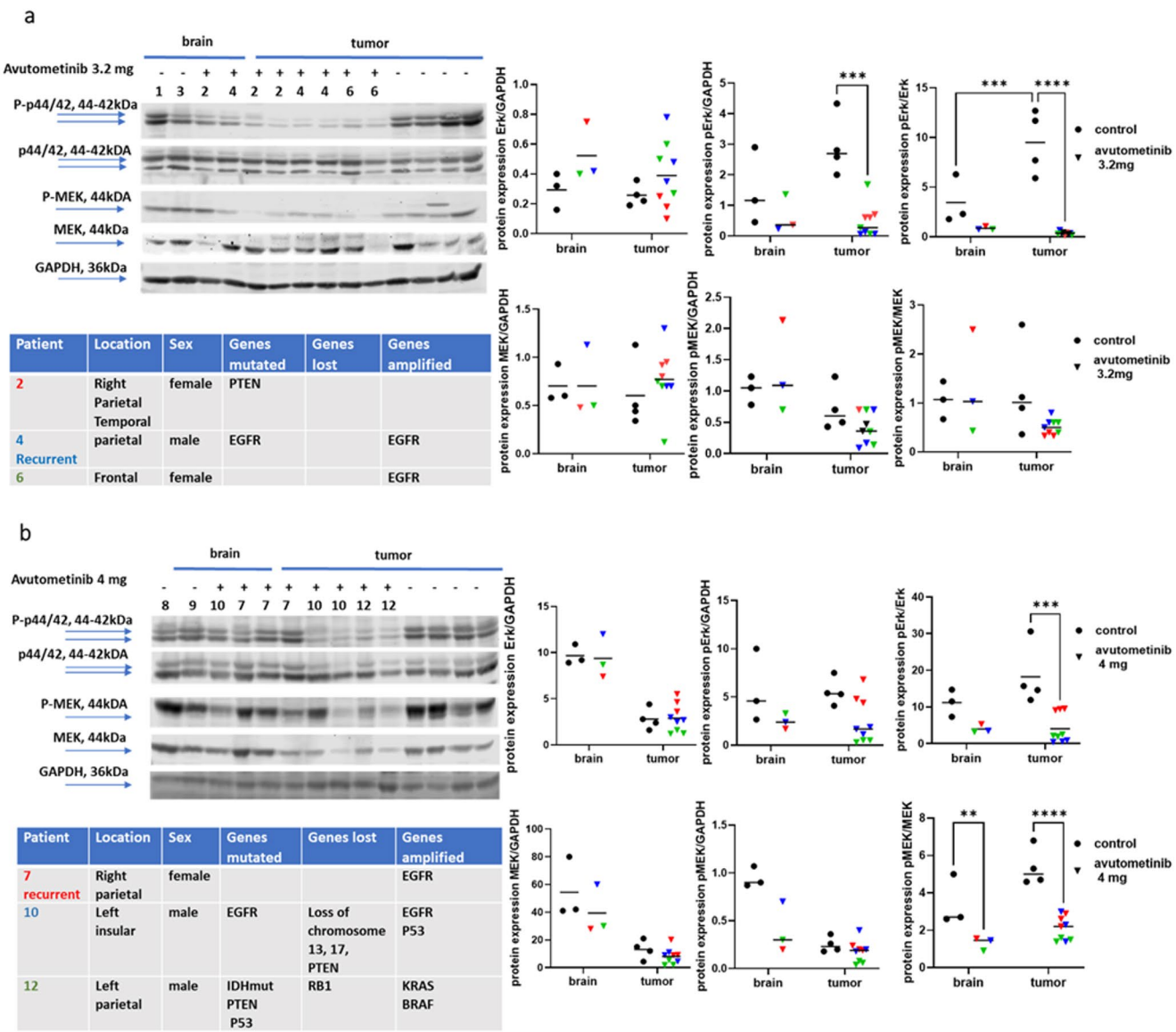

Patient	Location	Sex	Genes mutated	Genes lost	Genes amplified
2	Right Parietal Temporal	female	PTEN		
4 Recurrent	parietal	male	EGFR		EGFR
6	Frontal	female			EGFR

Patient	Location	Sex	Genes mutated	Genes lost	Genes amplified
7 recurrent	Right parietal	female			EGFR
10	Left insular	male	EGFR	Loss of chromosome 13, 17, PTEN	EGFR P53
12	Left parietal	male	IDHmut PTEN P53	RB1	KRAS BRAF

Fig. 3 Avutometinib at a dose of 3.2 mg reduced Erk phosphorylation, while scaling to 4 mg additionally resulted in downregulation of MEK phosphorylation in both tumors and the adjacent brain. Representative western blots and quantitative results for total and phosphorylated Erk1/2[Thr202/Tyr204] and MEK1/2[Ser217/221] are presented for avutometinib treatment at doses of 3.2mg (**a**) and 4mg (**b**). The degree of phosphorylation was calculated as the ratio of phosphorylated Erk or MEK to total Erk or MEK protein expression. Three samples taken from different areas of each tumor (proximal, median, and distal) were analyzed. Each color represents samples from the same tumor (distant, median, and proximal) and black circles correspond to untreated control samples. Patient data, tumor location, and tumor genetic phenotype based on pathology report, including tumor mutation panel and microarray RNA seq data, are provided. The values are shown as means ± SD. $^{**}p<0.01$, $^{***}p<0.001$, $^{****}p<0.0001$

A non-significant 2-fold reduction in p-FAK (Tyr925) expression was detected following 400 mg defactinib administration (predicted mean difference of 0.04), with no measurable effect observed in tumor-adjacent brain tissue.

Substantial variability in both total and phosphorylated Pyk2 and FAK levels was noted across tumor specimens and adjacent brain tissues, depending on tumor location and sampling site within the same tumor. Notably, among the 200 mg defactinib-treated group, tumors harboring PTEN mutations (samples #1 and #5), as well as the occipital tumor (sample #5), exhibited the highest levels of Pyk2 phosphorylation. However, all three tumors analyzed following 400 mg defactinib administration showed effective reductions in Pyk2 phosphorylation, regardless of genetic background, including those with PTEN mutations.

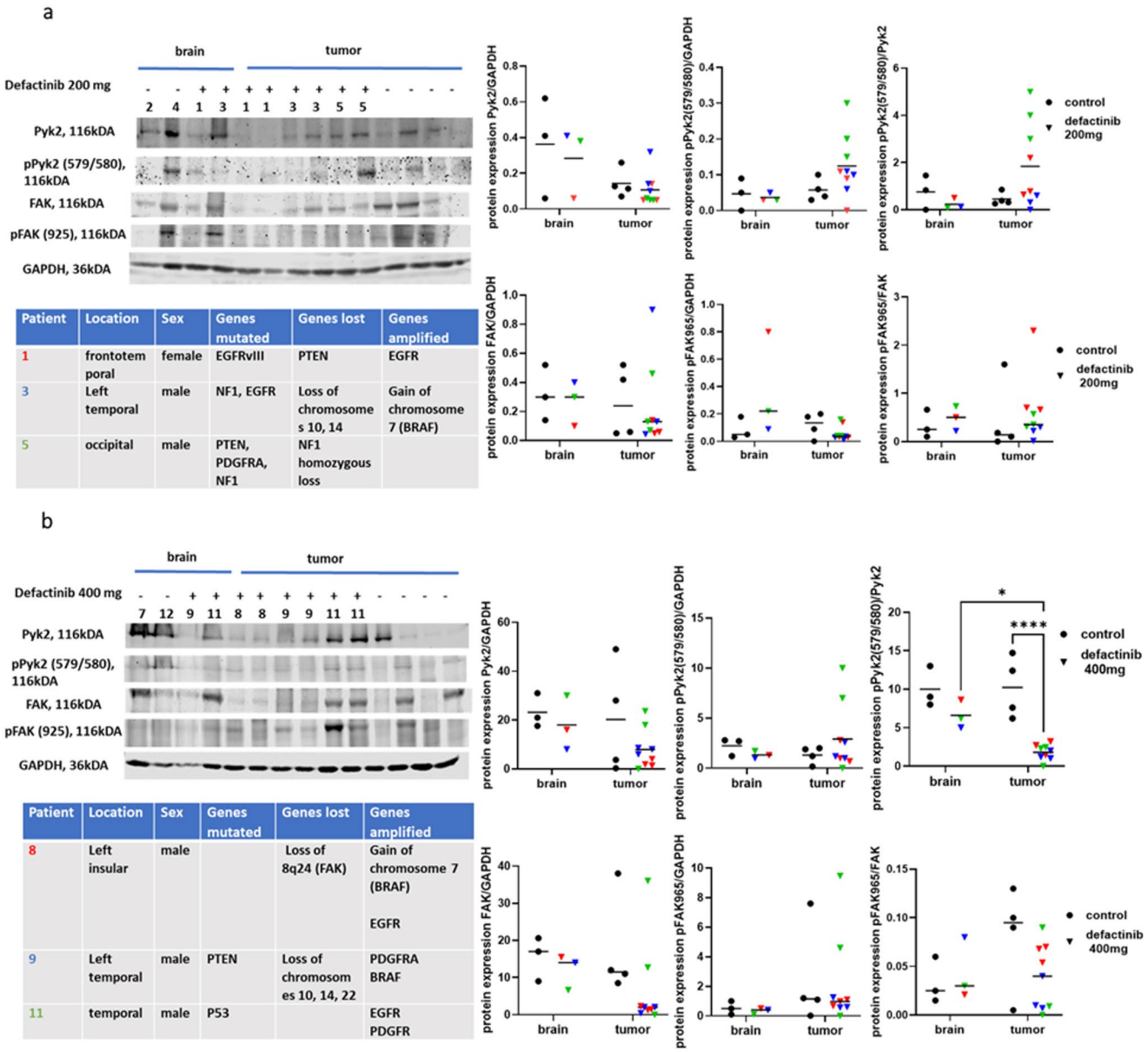

Patient	Location	Sex	Genes mutated	Genes lost	Genes amplified
1	frontotemporal	female	EGFRvIII	PTEN	EGFR
3	Left temporal	male	NF1, EGFR	Loss of chromosomes 10, 14	Gain of chromosome 7 (BRAF)
5	occipital	male	PTEN, PDGFRA, NF1	NF1 homozygous loss	

Patient	Location	Sex	Genes mutated	Genes lost	Genes amplified
8	Left insular	male		Loss of 8q24 (FAK)	Gain of chromosome 7 (BRAF) EGFR
9	Left temporal	male	PTEN	Loss of chromosomes 10, 14, 22	PDGFRA BRAF
11	temporal	male	P53		EGFR PDGFR

Fig. 4 Defactinib at a dose of 400 mg reduced Pyk2 phosphorylation without a significant effect on FAK phosphorylation levels. Representative western blots and quantitative results for total and phosphorylated Pyk2[Thr579/580] and FAK[Thr925] are presented for defactinib treatment at dose of 200mg (**a**) and 400mg (**b**). The degree of phosphorylation was calculated as the ratio of phosphorylated Pyk2 or FAK to the total Pyk2 or FAK protein expression. Three samples taken from different areas of each tumor (proximal, median, and distal) were analyzed. Each color represents samples from the same tumor (distant, median, and proximal). Patient data, tumor location, and tumor genetic phenotype based on the pathology report, including tumor mutation panel and microarray RNA seq data, are provided. The values are shown as means ± SD. *$p < 0.05$, ****$p < 0.0001$

Toxicity report and summary

The adverse events observed during the study were attributed to the effects of surgery and the underlying tumor and were not related to either investigational drug. A summary of these events is provided in Online Resource 7.

Discussion

In counseling sessions for patients with suspected GBMs, responses regarding estimated survival are often overly optimistic, based on outcomes from idealized clinical trial populations. Data from the most recent Central Brain Tumor Registry of the United States (CBTRUS) indicate that, in the broader population, average overall survival remains

only nine months—little changed from previous decades [36]. While advances in GBM biology continue to extend our understanding of this disease [37–39], these have not yet translated into a cure. Preclinical models can provide important mechanistic insight but rarely predict therapeutic success in humans [40]. Thus, rigorous evaluation of new agents, from early-stage studies such as this pilot to pivotal phase III trials, remains essential for meaningful clinical progress.

This pilot study provides exploratory evidence that both avutometinib and defactinib reach GBM tumor tissue and can modulate target signaling when administered orally prior to surgical resection. Avutometinib, a MEK/Erk inhibitor, significantly reduced Erk1/2 phosphorylation in GBM tumors at a 3.2 mg oral dose, confirming effective target engagement. No further reduction was observed at 4 mg, suggesting a saturation effect, with interpatient variability likely contributing in this small cohort. For example, tumor sample #7 (4 mg) showed the weakest response and was derived from a recurrent tumor, whereas another recurrent tumor, sample #4 (3.2 mg), exhibited a strong response comparable to newly diagnosed tumors. Both shared similar genetic features, including EGFR amplification. While sample size is limited, these observations highlight the potential influence of tumor microenvironment and signaling alterations in recurrent GBM on drug sensitivity.

Defactinib, a Pyk2/FAK inhibitor, demonstrated minimal effects on target phosphorylation at 200 mg but achieved notable inhibition of Pyk2 phosphorylation at 400 mg, irrespective of PTEN, PDGFR, or EGFR status. Changes in FAK phosphorylation remained modest and non-significant. The high variability in Pyk2 and FAK expression, both between patients and across tumor regions, coupled with the small sample size, limits definitive conclusions regarding defactinib pharmacodynamics. Nonetheless, these data provide initial insight into the heterogeneity of FAK/Pyk2 signaling in human GBM and suggest directions for future studies incorporating larger cohorts and diverse tumor regions.

Both agents exhibited limited pharmacodynamic effects in peritumoral brain tissue, indicating a degree of tumor-selective activity. For defactinib, little or no parent drug or M4 metabolite reached surrounding brain, and M2 metabolite concentrations were low relative to tumor tissue. Avutometinib levels in peritumoral brain were slightly higher, but this did not produce measurable effects on p-Erk1/2 or p-MEK1/2.

Taken together, these results should be interpreted as exploratory due to the small sample size and high intra- and inter-tumoral heterogeneity. Nevertheless, they support the feasibility of pharmacodynamic evaluation in GBM within a pre-surgical window and provide a rationale for larger studies investigating MEK/ERK and PYK2/FAK inhibitors, alone or in combination, across a broader spectrum of GBM molecular subtypes and treatment contexts.

Study limitations

In prior studies in non-GBM tumor types, the maximum serum concentration (Cmax) after a single dose occurs at approximately 2 h, reaching 184.4 ng/mL (200 mg) and 552.6 ng/mL (425 mg) for defactinib, and 209 ng/mL (3.2 mg) and 247 ng/mL (4 mg) for avutometinib [41, 42]. In the current study, lower serum concentrations were observed (10–40 ng/mL for defactinib and undetectable levels for avutometinib), consistent with later sampling times (151–212 min post-dose) during the declining phase of the concentration–time curve. Serum drug levels also showed substantial interpatient variability, as reported in prior single-agent trials [29, 41].

Plasma, tumor-adjacent brain, and tumor samples were generally occurred at delayed time points due to procedural factors such as anesthesia induction, surgical preparation, and variability in tumor location, depth, and vascularity. These factors likely contributed to low or undetectable drug levels in some specimens. In addition, all subjects had received dexamethasone for at least 48 h prior to drug administration, which may have induced CYP3A4 and accelerated the metabolism of both defactinib and avutometinib [43], with avutometinib appearing more sensitive to this effect. Therapeutic intratumoral concentrations for these agents in GBM remain unknown and will require dedicated clinical studies. Nevertheless, markedly higher drug levels in tumor tissue (up to 200 µg/mL for defactinib and up to 4 µg/mL for avutometinib) relative to serum indicate rapid and preferential tumor uptake.

GBM tumor tissue is highly heterogeneous, with regions varying from necrotic or liquefied to solid, gliotic, or highly vascularized. This heterogeneity likely influences both drug uptake and pharmacodynamic effects on target phosphorylation. Samples were collected from three separate regions per tumor to partially address this variability, but this approach cannot fully control for the intrinsic heterogeneity, which may explain the limited differences in drug concentrations observed despite administration of different doses.

No measurable pharmacodynamic effect was observed in the tumor-infiltrated brain adjacent to the resected GBM. This likely reflects low local drug exposure after a single dose and the predominance of normal brain tissue over tumor cells in these samples, which reduces assay sensitivity. Both avutometinib and defactinib are substrates of efflux transporters P-glycoprotein and breast cancer resistance protein, similar to other MEK and FAK/PYK2 inhibitors [44–45], which limits blood–brain barrier (BBB)

penetration. In contrast, abnormal vascularization and BBB disruption within GBM tumors may facilitate greater drug accumulation in tumor tissue relative to surrounding brain.

Taken together, these factors highlight the exploratory nature of this study. The small sample size, heterogeneous tissue, variable plasma exposure, and single-dose design limit definitive quantitative conclusions, but the findings provide important proof-of-concept evidence that both drugs can reach GBM tumors and produce measurable pharmacodynamic effects. Future studies with more frequent dosing, larger cohorts, and optimized sampling strategies will be essential to confirm and extend these observations.

Conclusions

After a single preoperative dose, both defactinib and avutometinib were detectable in GBM tumors. Despite the small cohort, exploratory analyses revealed measurable effects on their respective targets: avutometinib reduced Erk1/2 phosphorylation by approximately 28-fold, while defactinib decreased Pyk2 phosphorylation by 5.7-fold. Avutometinib was detected more frequently in tumor-adjacent brain tissue than defactinib, but neither drug induced significant changes in peritumoral tissue.

These findings support further investigation of these agents in GBM. They demonstrate that both drugs and relevant metabolites can reach tumors after a single dose and modulate intended molecular targets, providing proof-of-concept for target engagement in human GBM. Future studies could include additional presurgical "window-of-opportunity" evaluations, phase I studies of each agent alone, or dosing regimens informed by prior clinical experience in other cancers.

Importantly, this study illustrates that even a single preoperative dose can produce measurable biological effects in GBM tissue—a milestone rarely achieved in brain tumors. While the sample size is limited, these results highlight the feasibility and value of presurgical studies for assessing drug penetration and pharmacodynamic activity. Such exploratory, mechanism-driven approaches may guide the rational development of therapies and help overcome long-standing barriers to effective treatment in this aggressive disease.

Supplementary Information The online version contains supplementary material available at https://doi.org/10.1007/s00280-026-04870-4.

Acknowledgements The authors would like to thank Ryan Hanula for his assistance in study coordination, Jeffrey Switchenko of the Biostatistics Shared Resource at the Winship Cancer Institute for his assistance with statistical design, and the members of the Emory Integrated Metabolomics and Lipidomics Core for their work on developing the methods for measuring defactinib and avutometinib concentrations.

Author contributions L.K., M.M.V., and J.O. wrote the main manuscript text. M.M.V. prepared Figs. 1 and 2. L.K. prepared Figs. 3 and 4. J.O. prepared Table 1, and 2. J.O. coordinated patient enrollment and clinical trial procedures and activities. E.M.C. performed molecular analysis studies. K.K. and K.M-S performed mass-spectrometry metabolomic analysis. All authors reviewed the manuscript.

Funding This investigation was funded by a research grant from Verastem, Inc and Puerto Rico Science, Technology & Research Trust grant number PRSTRT2022. The authors have no financial or non-financial conflicts of interest. Informed consent was obtained from all subjects included in the study and the research was carried out with the continuous approval of Emory University Institutional Review Board approval: IRB#: STUDY00004876. At the UCC use of unidentifiable tissue samples was approved by the UCC Institutional Review Board Human Research Subject Protection Office (protocol # 2023-11). Additionally, the study was carried out under the Food and Drug Administration IND#: 164305. The study was registered on March 3, 2023 with ClinicalTrials.gov as NCT05798507. The first author received salary support via the Winn Diversity Career Development Award and the R25 MD007607 - Hispanic Clinical and Translational Research Education and Career Development Program.

Data availability No datasets were generated or analysed during the current study.

Declarations

Competing interests Lilia Kucheryavykh has received research support from Puerto Rico Science, Technology & Research Trust grant number PRSTRT2022. Jeffrey Olson has received funding for the conduct of this study from Verastem, Inc. Miguel Mayol del Valle has received salary support and training from Winn Diversity Career Development Award; Hispanic Center of Excellence, travel support from Hispanic Center of Excellence Research Fellowship Program, and speaker compensation from AHOMPR 2024 Annual Meeting.

References

1. Price M, Ballard C, Benedetti J et al (2024) CBTRUS statistical report: primary brain and other central nervous system tumors diagnosed in the united States in 2017–2021. Neuro-oncol 26(6):vi1–vi85. https://doi.org/10.1093/neuonc/noae145

2. Mellinghoff IK, van den Bent MJ, Blumenthal DT et al (2023) Vorasidenib in IDH1- or IDH2-Mutant Low-Grade glioma. N Engl J Med 389:589–601. https://doi.org/10.1056/NEJMoa2304194
3. Yan H, Parsons DW, Jin G et al (2009) IDH1 and IDH2 mutations in gliomas. New Engl J Med 360:765–773. https://doi.org/10.1056/NEJMoa0808710
4. Gilbert MR, Dignam JJ, Armstrong TS et al (2014) A randomized trial of bevacizumab for newly diagnosed glioblastoma. N Engl J Med 370:699–708. https://doi.org/10.1056/NEJMoa1308573
5. Chinot OL, Wick W, Mason W et al (2014) Bevacizumab plus Radiotherapy-Temozolomide for newly diagnosed glioblastoma. N Engl J Med 370:709–722. https://doi.org/10.1056/NEJMoa1308345
6. Rich JN, Reardon DA, Peery T et al (2004) Phase II trial of gefitinib in recurrent glioblastoma. J Clin Oncol 22:133–142. https://doi.org/10.1200/JCO.2004.08.110
7. Hegi ME, Diserens AC, Bady P et al (2011) Pathway analysis of glioblastoma tissue after preoperative treatment with the EGFR tyrosine kinase inhibitor gefitinib–a phase II trial. Mol Cancer Ther 10:1102–1112. https://doi.org/10.1158/1535-7163.MCT-11-0048
8. Fougner V, Hasslebach B, lassen U et al (2022) Implementing targeted therapies in the treatment of glioblastoma: previous shortcomings, future promises, and a multimodal strategy recommendation. Neuro-oncol Adv 4:1–11. https://doi.org/10.1093/noajnl/vdac157
9. Stupp R, Hegi ME, Gilbert MR, Chakravarti A (2007) Chemoradiotherapy in malignant glioma: standard of care and future directions. J Clin Oncol 25:4127–4136. https://doi.org/10.1200/JCO.2007.11.8554
10. Vogelbaum: Vogelbaum MA, Krivosheya D, Borghei-Razavi H et al (2020) Phase 0 and window of opportunity clinical trial design in neuro-oncology: a RANO review. Neuro-Oncol 22:1568–1579. https://doi.org/10.1093/neuonc/noaa149
11. Robinson JP, VanBrocklin MW, Guilbeault AR, Signorelli DL, Brandner S, Holmen SL (2010) Activated BRAF induces gliomas in mice when combined with Ink4a/Arf loss or Akt activation. Oncogene 29:335–344. https://doi.org/10.1038/onc.2009.333
12. Nuñez RE, Del Valle MM, Ortiz K, Almodovar L, Kucheryavykh L (2021) Microglial cytokines induce invasiveness and proliferation of human glioblastoma through Pyk2 and FAK activation. Cancers (Basel) 13(24):6160. https://doi.org/10.3390/cancers13246160
13. Makino Y, Arakawa Y, Yoshioka E, Shofuda T, Minamiguchi S, Kawauchi T et al (2021) Infrequent RAS mutation is not associated with specific histological phenotype in gliomas. BMC Cancer 21(1):1025. https://doi.org/10.1186/s12885-021-08733-4
14. Andrews LJ, Thornton ZA, Saincher SS, Yao IY, Dawson S, McGuinness LA et al (2022) Prevalence of BRAFV600 in glioma and use of BRAF inhibitors in patients with BRAFV600 mutation-positive glioma: systematic review. Neuro Oncol 24:528–540. https://doi.org/10.1093/neuonc/noab247
15. Lyustikman Y, Momota H, Pao W, Holland E (2008) Constitutive activation of Raf-1 induces glioma formation in mice. Neoplasia 10(5):501–510. https://doi.org/10.1593/neo.08206
16. Verhaak RG, Hoadley KA, Purdom E, Wang V, Qi Y, Wilkerson MD et al (2010) Integrated genomic analysis identifies clinically relevant subtypes of glioblastoma characterized by abnormalities in PDGFRA, IDH1, EGFR, and NF1. Cancer Cell 17:98–110. https://doi.org/10.1016/j.ccr.2009.12.020
17. Xiaojing Wang S, Min H, Liu N, Wu X, Liu T, Wang W, Li Y, Shen H, Wang Z, Qian H, Xu C, Zhao Y, Chen (2019) Nf1 loss promotes Kras-driven lung adenocarcinoma and results in Psat1-mediated glutamate dependence. EMBO Mol Med 11(6):e9856. https://doi.org/10.15252/emmm.201809856
18. Khan S, Martinez-Ledesma E, Dong J, Mahalingam R, Park SY, Piao Y, Koul D, Balasubramaniyan V, de Groot JF, Yung WKA (2023) Neuronal differentiation drives the antitumor activity of mitogen-activated protein kinase kinase (MEK) inhibition in glioblastoma. Neurooncol Adv 5(1):vdad132. https://doi.org/10.1093/noajnl/vdad132
19. McNeill RS, Canoutas DA, Stuhlmiller TJ, Dhruv HD, Irvin DM, Bash RE, Angus SP, Herring LE, Simon JM, Skinner KR, Limas JC, Chen X, Schmid RS, Siegel MB, Van Swearingen AED, Hadler MJ, Sulman EP, Sarkaria JN, Anders CK, Graves LM, Berens ME, Johnson GL, Miller CR (2017) Combination therapy with potent PI3K and MAPK inhibitors overcomes adaptive kinome resistance to single agents in preclinical models of glioblastoma. Neuro Oncol 19(11):1469–1480. https://doi.org/10.1093/neuonc/nox044
20. Deramaudt TB, Dujardin D, Hamadi A, Noulet F, Kolli K, De Mey J et al (2011) FAK phosphorylation at Tyr-925 regulates cross-talk between focal adhesion turnover and cell protrusion. Mol Biol Cell Apr 22(7):964–975
21. Lipinski CA, Tran NL, Bay C, Kloss J, McDonough WS, Beaudry C, Berens ME, Loftus JC (2003) Differential role of proline-rich tyrosine kinase 2 and focal adhesion kinase in determining glioblastoma migration and proliferation. Mol Cancer Res Mar 1(5):323–332 PMID: 12651906
22. Loftus JC, Yang Z, Tran NL, Kloss J, Viso C, Berens ME, Lipinski CA (2009) The Pyk2 FERM domain as a target to inhibit glioma migration. Mol Cancer Ther Jun 8(6):1505–1514. https://doi.org/10.1158/1535-7163.MCT-08-1055Epub 2009 Jun 9. PMID: 19509258; PMCID: PMC3180876
23. Lipinski CA, Tran NL, Menashi E, Rohl C, Kloss J, Bay RC, Berens ME, Loftus JC (2005) The tyrosine kinase pyk2 promotes migration and invasion of glioma cells. Neoplasia May 7(5):435–445. https://doi.org/10.1593/neo.04712PMID: 15967096; PMCID: PMC1501165
24. Hecker TP, Ding Q, Rege TA, Hanks SK, Gladson CL (2004) Overexpression of FAK promotes Ras activity through the formation of a FAK/p120RasGAP complex in malignant Astrocytoma cells. Oncogene 23:3962–3971
25. Rolón-Reyes K, Kucheryavykh YV, Cubano LA, Inyushin M, Skatchkov SN, Misty J, Eaton MJ et al (2015) Microglia Activate Migration of Glioma Cells through a Pyk2 Intracellular Pathway. PLoS One 10(6):e0131059 https://doi.org/10.1371/journal.pone.0131059
26. Ortiz–Rivera J, Nuñez R, Kucheryavykh Y, Kucheryavykh L (2023) The PYK2 inhibitor PF–562271 enhances the effect of Temozolomide on tumor growth in a C57Bl/6–Gl261 mouse glioma model. J Neurooncol Feb 161(3):593–604. https://doi.org/10.1007/s11060-023-04260-3
27. Ortiz Rivera J, Velez Crespo G, Inyushin M et al (2023) Pyk2/FAK signaling is upregulated in recurrent glioblastoma tumors in a C57BL/6/GL261 glioma implantation model. Int J Mol Sci 24:13467. https://doi.org/10.3390/ijms241713467
28. McNamara B, Demirkiran C, Hartwich TMP et al (2024) Preclinical efficacy of RAF/MEK clamp Avutometinib in combination with FAK Inhibition in low grade serous ovarian cancer. Gynecol Oncol 183:133–140. https://doi.org/10.1016/j.ygyno.2024.01.028
29. Banerjee S, Krebs MG, Greystoke A Defactinib with avutometinib in patients with solid tumors: the phase 1 FRAME trial. Nat Med 31: 3074–3080 (2025)., Jackson GA, Adamson DC et al (2025) (2025) Similarities in Mechanisms of Ovarian Cancer Metastasis and Brain Glioblastoma Multiforme Invasion Suggest Common Therapeutic Targets. Cells 14:171 https://doi.org/10.3390/cells14030171
30. Cloughesy TF, Wen PY, Robins HI, Chang SM, Groves MD, Fink KL, Junck L, Schiff D, Abrey L, Gilbert MR, Lieberman F,

Kuhn J, DeAngelis LM, Mehta M, Raizer JJ, Yung WK, Aldape K, Wright J, Lamborn KR, Prados MD (2006) Phase II trial of Tipifarnib in patients with recurrent malignant glioma either receiving or not receiving enzyme-inducing antiepileptic drugs: a North American brain tumor consortium study. J Clin Oncol 24:3651–3656. https://doi.org/10.1200/JCO.2006.06.2323

31. Liu J, Xue L, Xu X, Luo J, Zhang S (2021) FAK-targeting PROTAC demonstrates enhanced antitumor activity against KRAS mutant non-small cell lung cancer. Exp Cell Res 408(2):112868. https://doi.org/10.1016/j.yexcr.2021.112868
32. Hirata E, Girotti MR, Viros A, Hooper S, Spencer-Dene B, Matsuda M, Larkin J, Marais R, Sahai E (2015) Intravital imaging reveals how BRAF Inhibition generates drug-tolerant microenvironments with high integrin beta1/FAK signaling. Cancer Cell 13(4):574–588. https://doi.org/10.1016/j.ccell.2015.03.008
33. Banerjee S, Grochet R, Shinde R et al (2021) Phase I study of the combination of the dual RAF/MEK inhibitor VS-6766 and the FAK inhibitor defactinib: results of efficacy in low grade serous ovarian cancer. Ann Oncol 32(Supplement 5):S728 Meeting Abstract
34. Sagerer A, Eyüpoglu IY, Juratli TA, Cordes N (2025) Context-specific targeting of focal adhesion kinase in brain tumors: lessons from glioblastoma and neurofibromatosis type 2-mutant meningioma. Front Oncol 15:1724278. https://doi.org/10.3389/fonc
35. Furqan M, Elliott RJR, Nagle PWK, Dawson JC, Masalmeh R, Garcia VA, Munro AF, Drake C, Morrison GM, Pollard SM, Ebner D, Brunton VG, Frame MC, Carragher NO (2025) Drug Combinations Targeting FAK and MEK Overcomes Tumor Heterogeneity in Glioblastoma. Pharmaceutics 17(5):549. https://doi.org/10.3390/pharmaceutics17050549
36. Price M, Ballard C, Benedetti J, Neff C, Cioffi G, Waite KA, Kruchko C, Barnholtz-Sloan JS, Ostrom QT (2024) CBTRUS Statistical Report: Primary Brain and Other Central Nervous System Tumors Diagnosed in the United States in 2017–2021, Neuro-Oncol, 26, Supplement 6, Pages vi1–vi85. https://doi.org/10.1093/neuonc/noae145
37. Pouyan A, Ghorbanlo M, Eslami M, Jahanshahi M, Ziaei E, Salami A, Hashemi M (2025) Glioblastoma multiforme: insights into pathogenesis, key signaling pathways, and therapeutic strategies. Mol Cancer 24(1):58. https://doi.org/10.1186/s12943-025-02267-0
38. Hasan S, Mahmud Z, Hossain M, Islam S (2024) Harnessing the role of aberrant cell signaling pathways in glioblastoma multiforme: a prospect towards the targeted therapy. Mol Biol Rep 51(1):1069. https://doi.org/10.1007/s11033-024-09996-3
39. Zeller SL, Spirollari E, Chandy AM, Hanft SJ, Gandhi CD, Jhanwar-Uniyal M (2024) Understanding the genomic landscape of glioblastoma: opportunities for targeted therapies. Anticancer Res 44:4677–4690. https://doi.org/10.21873/anticanres.17295
40. Pasupuleti V, Vora L, Prasad R, Nandakumar DN, Khatri DK (2024) Glioblastoma preclinical models: strengths and weaknesses. Biochim Biophys Acta Rev Cancer Jan 1879(1):189059. https://doi.org/10.1016/j.bbcan.2023.189059
41. Guo C, Chénard-Poirier M, Roda D, de Miguel M, Harris SJ, Candilejo IM, Sriskandarajah P, Xu W, Scaranti M, Constantinidou A, King J, Parmar M, Turner AJ, Carreira S, Riisnaes R, Finneran F, Hall E, Ishikawa Y, Nakai K, Tunariu N, Basu B, Kaiser M, Lopez JS, Minchom A, de Bono JS, Banerji U (2020) Intermittent schedules of the oral RAF–MEK inhibitor CH5126766/VS-6766 in patients with RAS/RAF-mutant solid tumours and multiple myeloma: a single-centre, open-label, phase 1 dose-escalation and basket dose-expansion study. Lancet Oncol 21:1478–1488. https://doi.org/10.1016/S1470-2045(20)30464-2
42. Jones SF, Siu LL, Bendell JC, Cleary JM, Razak ARA, Infante JR, Pandya SS, Bedard PL, Pierce KJ, Houk B, Roberts WG, Shreeve SM, Shapiro GI (2015) A phase I study of VS-6063, a second-generation focal adhesion kinase inhibitor, in patients with advanced solid tumors. Invest New Drugs 33:1100–1107. https://doi.org/10.1007/s10637-015-0282-y
43. Bourdin V, Bigot W, Vanjak A, Burlacu R, Lopes A, Champion K, Depond A, Amador-Borrero B, Sene D, Comarmond C et al (2023) Drug–Drug interactions involving dexamethasone in clinical practice: myth or reality? J Clin Med 12:7120. https://doi.org/10.3390/jcm12227120
44. Brown NF, Williams M, Arkenau HT, Fleming RA, Tolson J, Yan L, Zhang J, Singh R, Auger KR, Lenox L, Cox D, Lewis Y, Plisson C, Searle G, Saleem A, Blagden S, Mulholland P (2018) A study of the focal adhesion kinase inhibitor GSK2256098 in patients with recurrent glioblastoma with evaluation of tumor penetration of [11 C]GSK2256098. Neuro Oncol 20(12):1634–1642. https://doi.org/10.1093/neuonc/noy078
45. Vaidhyanathan S, Mittapalli RK, Sarkaria JN, Elmquist WF (2014) Factors influencing the CNS distribution of a novel MEK-1/2 inhibitor: implications for combination therapy for melanoma brain metastases. Drug Metab Dispos Aug 42(8):1292–1300. https://doi.org/10.1124/dmd.114.058339